Longitudinal double helicity asymmetry A_{LL} from direct photon, jet and charged pion production in polarized $\vec{p}+\vec{p}$ collisions

Zhongling Ji[1⋆] for the PHENIX Collaboration

1 Stony Brook University

⋆ zhongling.ji@stonybrook.edu

Proceedings for the XXVIII International Workshop on Deep-Inelastic Scattering and Related Subjects, Stony Brook University, New York, USA, 12-16 April 2021
doi:10.21468/SciPostPhysProc.8

Abstract

Understanding the proton spin composition from the quarks and gluons spin polarization and their motion is important to test various kinds of sum rules and nonperturbative properties of hadrons. At the Relativistic Heavy Ion Collider (RHIC), we collide longitudinally polarized proton beams and measure the double helicity asymmetry A_{LL}, which is an important physical quantity for extracting the polarized parton distribution functions (PDFs) of the proton. Direct photon, jet and charged pion production are good channels to probe the gluon spin polarization inside the proton, with the ability to probe also the sign of the gluon spin. Direct photon production is the theoretically "cleanest" channel, with little fragmentation contribution, but limited by statistics. On the other hand, jet and charged pion production have more statistics, but include more hard processes and hadronization effects. I will present the recent measurements of direct photon, jet and charged pion A_{LL}s at PHENIX and show their complementary roles in extracting the gluon spin.

Received 30-07-2021
Accepted 06-05-2022
Published 13-07-2022
doi:10.21468/SciPostPhysProc.8.090

1 Introduction

Nucleons (protons and neutrons) and electrons are the building block of the ordinary matters. While electrons are taken as fundamental particles with point structure in the Standard Model (SM), protons and neutrons are composite particles with rich structures. These structures are usually revealed through high energy collisions and take partons (quarks and gluons) as the underlying degrees of freedom. One of the interesting structures is the longitudinal spin decomposition of the proton, which decomposes the proton spin as the spin and orbital momentum contributions from quarks and gluons

$$\frac{1}{2}=\frac{1}{2}\Delta\Sigma+\Delta G+L_q+L_g, \tag{1}$$

where $\frac{1}{2}\Delta\Sigma$ and ΔG are spin contributions from quarks and gluons, respectively, L_q and L_g are their orbital momentum contributions. The spin contributions can further be expressed based on longitudinal momentum fractions of partons

$$\Delta\Sigma = \sum_{q=u,d,s} \int_0^1 \Delta q(x) dx, \tag{2}$$

$$\Delta G = \int_0^1 \Delta g(x) dx, \tag{3}$$

where $x = p^+/P^+$ is the fraction of longitudinal momentum carried by the parton and P^+ (p^+) is the proton's (parton's) momentum in the light cone frame.

The polarized inclusive deep inelastic scattering (pDIS) [1–4] probes the singlet axial charge $g_A^{(0)}$, which is related to parton spin

$$g_A^{(0)}|_{\text{pDIS}} = \Delta\Sigma - 3\frac{\alpha_s}{2\pi}\Delta G, \tag{4}$$

where α_s is the strong coupling constant. The polarized semi-inclusive deep inelastic scattering (pSIDIS) probes the gluon spin $\Delta g(x)$ through next-to-leading order (NLO) photon-gluon fusion process $\gamma^* g \to q\bar{q}$ [5,6]. The longitudinal polarized proton-proton collisions can probe the gluon spin at leading order (LO). Currently, the Relativistic Heavy Ion Collider (RHIC) is the only machine capable of colliding polarized proton beams [7]. Measurements of double helicity asymmetry (A_{LL}) of direct photon, jet and charged pion productions in polarized $\vec{p}+\vec{p}$ collisions are three complementary channels to probe the gluon spin inside the proton. Direct photon with an isolation criterion is mainly produced by quark-gluon Compton scattering $qg \to q\gamma$. Since there is little fragmentation contribution to the direct photon production, this is the "cleanest" channel. But it is limited by statistics due to the suppression by the electromagnetic coupling constant. On the other hand, the jet and charged pion productions probe the gluon spin through $qg \to qg$ and $gg \to gg$ scatterings, which have more statistics, but are influenced more by hadronization processes. In addition, the charged pion productions have the ability to separate the u and d quark contributions. Recent RHIC measurements of π^0 and jets at $\sqrt{s} = 62.4$ and 200 GeV [8–12] included in global analyses have shown the first direct evidence of nonzero gluon spin contributions to the spin of the proton [13, 14] in the Bjorken-x range larger than 0.05. Measurements at higher energy $\sqrt{s} = 510$ GeV [15, 16] have confirmed the nonzero gluon polarization and extended the minimum x reach to ~0.01. I will present the recent PHENIX spin measurements from direct photon, jet and charged pion.

2 Experimental setup

The measurements of direct photon, jet and charged pion A_{LL} are taken at $\sqrt{s} = 510$ GeV from the 2013 RHIC running period by the PHENIX detector [17] in midrapidity, which has pseudorapidy coverage $|\eta| < 0.35$ and π coverage for azimuthal angle ϕ. The primary detector for high energy photons is an electromagnetic calorimeter (EMCal) [18], consisting of two subsystems, a six sector lead-scintillator (PbSc), and a two sector lead glass (PbGl) detector, each located 5 m radially from the beam line. The EMCal has fine granularity with each tower covering $\Delta\eta \times \Delta\phi \sim 0.01 \times 0.01$ (0.008×0.008) for PbSc (PbGl). The high energy photons are selected by an EMCal trigger, which combines each 4×4 towers of EMCal to a single module and requires an energy threshold ranging from 3.7 to 5.6 GeV. The Drift Chamber (DC) [19] is used to measure the momentum of charged particles in jet and charged pions and veto charged particles in direct photon measurements. The Pad Chamber 3 (PC3) is used to

match the DC track in the jet measurement. The Ring Čerenkov detector (RICH) [20] is used for particle identification (PID) of charged pions. The Beam-Beam Counters (BBC) [21] cover $3.1 < |\eta| < 3.9$ and are located at ±144 cm from the interaction point along the beam line. The BBCs measure the collision vertex and provide a minimum-bias (MB) trigger. The BBCs are also used as a luminosity monitor.

The observed physical quantity is the double helicity asymmetry A_{LL}, which is defined as

$$A_{LL} = \frac{\Delta\sigma}{\sigma} = \frac{\sigma_{++} - \sigma_{+-}}{\sigma_{++} + \sigma_{+-}}, \tag{5}$$

where σ_{++} (σ_{+-}) is the cross section for the same (opposite) helicity proton collisions. This can be rewritten in terms of particle yield and beam polarizations:

$$A_{LL} = \frac{1}{P_B P_Y} \frac{N_{++} - RN_{+-}}{N_{++} + RN_{+-}}, \tag{6}$$

where N_{++} (N_{+-}) is the number of measured events from the collisions with the same (opposite) helicities. P_B and P_Y are the polarizations for the two proton beams, and the average values in 2013 were 0.55 and 0.57, respectively [22]. R ($= \mathcal{L}_{++}/\mathcal{L}_{+-}$) is the relative luminosity that is measured by the BBC.

3 Direct photon A_{LL}

The sources of direct photon signal at leading order include: quark gluon Compton scattering $gq \to q\gamma$, quark antiquark annihilation $q\bar{q} \to g\gamma$, parton fragmentation to photon, and quark bremsstrahlung. The background photons mainly come from decay photons from hadrons, such as π^0, η, ω and η'. The photons are required to pass the EMcal trigger and measured by the EMCal. The π^0 can be reconstructed by the invariant mass of its two decay photons in the mass range $110 < M_{\gamma\gamma} < 160$ MeV/c^2 ($M_{\pi^0} \pm 3\sigma$). The production ratios of η, ω, η' over π^0 are obtained based on the previous $\sqrt{s} = 200$ GeV measurement [23]. To reduce the hadron decay background and the photons from parton fragmentation and quark bremsstrahlung, an isolation criteria is used. For any other particles within a cone of radius $r_{cone} = \sqrt{(\delta\eta)^2 + (\delta\phi)^2} = 0.5$ of the signal photon, the isolation criteria requires the energy sum of neutral particles in the EMCal plus the momentum sum of charged particles in the DC is less than 10% of the energy of the signal photon: $E_{cone} = E_{neutral} + p_{charged} \cdot c < 0.1E_\gamma$.

The isolated direct photon cross section at $|\eta| < 0.25$ in psudorapidity at $\sqrt{s} = 510$ GeV is shown in Fig. 1 as a function of p_T and compared with the JETPHOX NLO perturbative Quantum Chromodynamics (pQCD) calculation [24] using CT14 parton distribution functions (PDF) [25] and BFGII fragmentation function (FF) [26]. The calculation is in good agreement with our data within the uncertainties.

In Fig. 2, the ratio of isolated over inclusive direct photons is shown together with theoretical calculations. The MC simulations are from POWHEG + PYTHIA8 [27–31]. POWHEG is a NLO partonic level generator, the output of which can be used as the input for PYTHIA8. The PYTHIA8 includes the multiparton interactions (MPI), parton showers (PS) and fragmentation processes. POWHEG uses CT14 PDF [25]. There is no final-state factorization scale in PYTHIA8 as it uses string fragmentation instead. In the POWHEG+PYTHIA8 simulations, the uncertainties from renormalization and factorization scales are canceled between the numerator and denominator of the fraction. The JETPHOX NLO pQCD calculations overestimate the data due to its partonic nature. POWHEG+PYTHIA8 with MPI+PS gives better prediction for the isolated over inclusive direct photon cross section ratio.

The double helicity asymmetry of isolated direct photon production in longitudinally polarized proton collisions at $|\eta| < 0.25$ in psudorapidity at $\sqrt{s} = 510$ GeV is shown in Fig. 3

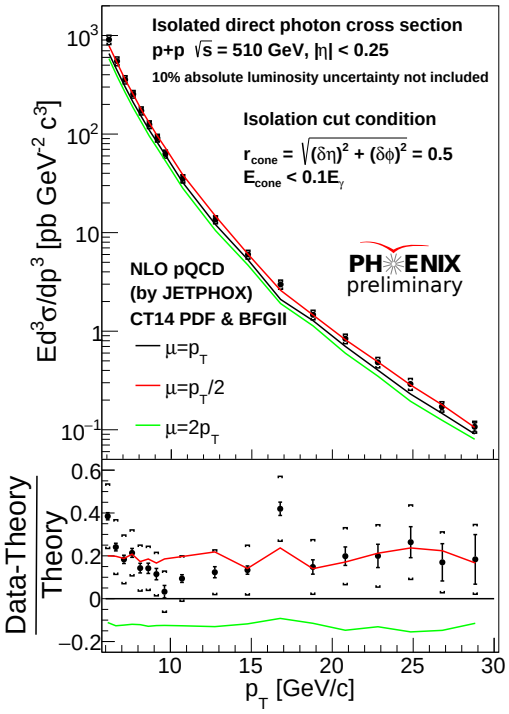

Figure 1: Isolated direct photon cross section as a function of p_T compared with JETPHOX NLO pQCD calculations [24] for different renormalization and factorization scales $\mu = p_T/2$ (dashed line), p_T (solid line), $2p_T$ (dotted line). The bars represent statistical uncertainties and square brackets are for systematic uncertainties. The bottom plot shows the comparison of data and calculations.

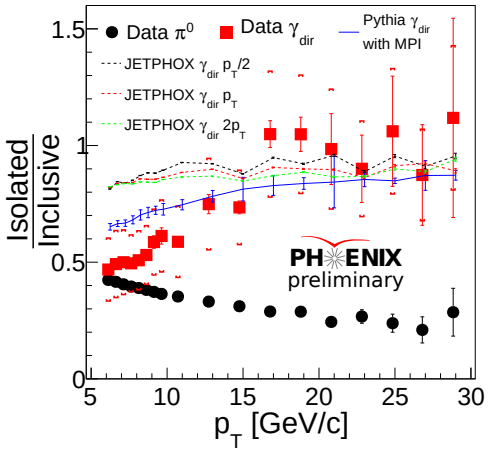

Figure 2: Isolated over inclusive direct photon ratio: bars are statistical uncertainties and square brackets are systematic uncertainties. POWHEG + PYTHIA8 without MPI and JETPHOX NLO pQCD calculations with different renormalization and factorization scales are also shown.

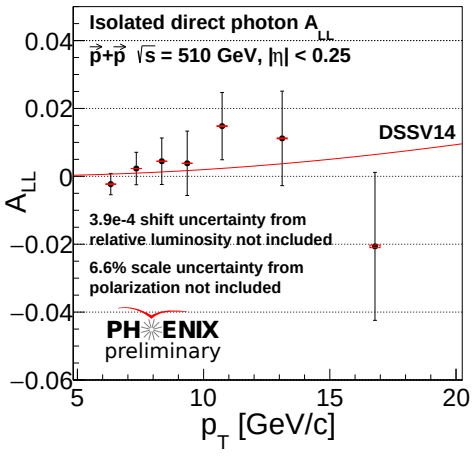

Figure 3: Double helicity asymmetry A_{LL} *vs* p_T for isolated direct photon production in polarized p+p collisions at $\sqrt{s} = 510$ GeV at midrapidity. Vertical error bars (boxes) represent the statistical (systematic) uncertainties. The NLO pQCD calculation at $\sqrt{s}$ = 500 GeV is plotted as the solid curve.

for $6 < p_T < 20$ GeV/c. The NLO pQCD calculation was obtained using DSSV14 polarized PDF, CT10 unpolarized PDF and GRV FF for the renormalization and factorization scales $\mu = p_T$ [13, 32, 33]. The calculation is in good agreement with our results within the experimental uncertainties. This result will provide new constraint on gluon spin ΔG when included in the global analysis in the future.

4 Jet A_{LL}

The jet measurements use the anti-k_T algorithm [34] with cone size R = 0.3 at $|\eta| < 0.15$ in psudorapidity at $\sqrt{s} = 510$ GeV. The momentum of charged particles is measured by the DC with a confirming match in PC3, while the energy of neutral particles is measured by the EMCal with a time-of-flight requirement to remove clusters from previous crossings due to the electronic device latency of EMCal. Good tracks and clusters are associated to avoid double counting. The selected events are required to pass the EMCal trigger with an energy threshold of 5.6 GeV. Only the jet with the largest p_T in the event is kept. The reconstructed p_T is unfolded to the true p_T by Bayes iteration method [35] implemented by RooUnfold.

Fig. 4 shows the measured jet cross section and comparison with NLO pQCD calculation with ln(R) resummations. The calculation largely overestimates the data. Such a behavior is seen also by CMS when having small R sizes [36].

Fig. 5 shows the jet A_{LL} measurement at PHENIX by using data from RHIC run 2013. The systematic uncertainties are correlated due to unfolding. The STAR jet A_{LL} measurement from RHIC run 2012 is also shown as a comparison. The theory calculation from NLO pQCD with ln(R) resummations and DSSV14 polarized PDF [13] is consistent with data. These measurements will provide independent constraint on polarized gluon PDF $\Delta g(x)$ when included in the global analysis in the future.

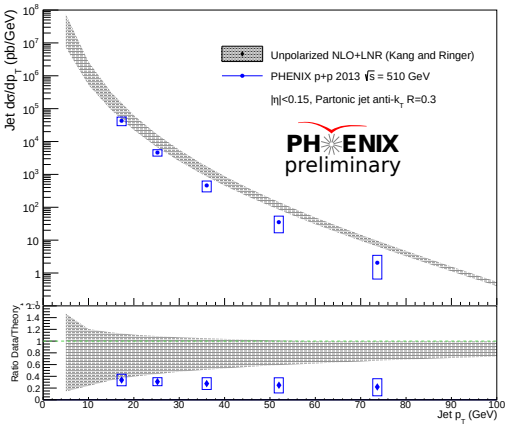

Figure 4: Jet cross section as a function of p_T compared with NLO pQCD calculations with ln(R) resummations. The bars represent statistical uncertainties and square brackets are for systematic uncertainties. The bottom plot shows the comparison of data and calculations.

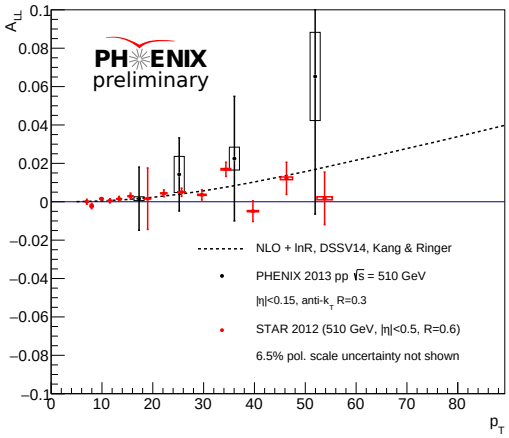

Figure 5: Jet A_{LL} as a function of p_T compared with NLO pQCD calculations with ln(R) resummations. The bars represent statistical uncertainties and square brackets are for systematic uncertainties. The measurement from RHIC run 2012 at STAR is shown as a comparison.

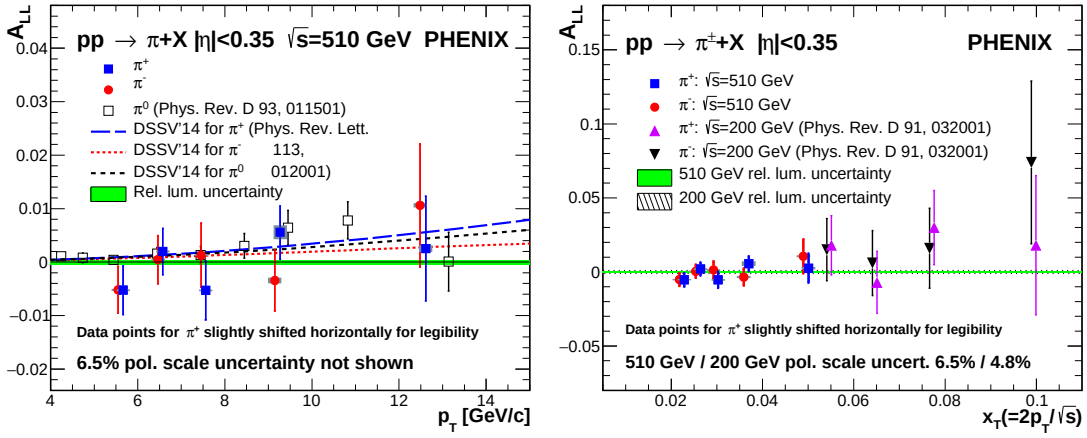

(a) A_{LL} vs p_T. A_{LL}'s of previously published neutral pions (open black squares) [15] and DSSV14 calculations [13] are also shown.

(b) A_{LL}'s of charged pions for positive (closed blue squares) and negative pions (closed red circles) at $\sqrt{s} = 510$ GeV. The statistical uncertainties of asymmetries and the point-to-point systematic uncertainties from background are represented by the continuous lines and the gray bands, respectively.

Figure 6: A_{LL} of charged pions.

5 Charged pion A_{LL}

The charged pions are measured at PHENIX at $|\eta| < 0.35$ in psudorapidity at $\sqrt{s} = 510$ GeV [37]. The particles are required to pass a preselection rule with cluster energy over reconstructed momentum ratio $0.2 < E/p < 0.8$, since the signal-to-background ratio is high in this range (fig. 4 of [37]). The preselected particles are required to fire the EMCal trigger. Only the small fraction of pions that shower already in the EMCAL get selected with this trigger. In addition to the trigger, the charged pion candidate track measured by the DC is required to be pointing to the EMCal tower that fired the trigger. RICH is used as an additional PID and more than one photomultiplier is required to be fired by the charged pion candidate with threshold of ∼4.9 GeV. The next threshold of RICH is 17.3 GeV from kaons. An EM shower shape requirement is also used to reduce electron background.

The A_{LL}'s of charged pions are shown in fig. 6a for p_T dependence and fig. 6b for x_T dependence. The measurements are consistent with calculations from DSSV14 [13]. From fig. 6b, we see that the data from 510 GeV probe lower x_T range. However, there is not enough statistics to decide whether π^+ or π^- has larger A_{LL}.

6 Conclusion

The proton spin decomposition is important to understand the nonperturbative structure of the proton and test various spin sum rules. The gluon spin $\Delta g(x)$ is particularly interesting, but it is not constrained well by existing pDIS and pSIDIS measurements. Longitudinal polarized protons at RHIC are capable of probing the gluon spin at leading order. The direct photon production provides the most "clean" probe to the gluon spin due to little fragmentation contributions involved. The jet and charged pions provide complementary probe to the proton spin with more statistics. Together with the PHENIX ongoing forward cluster and forward/central η measurements, these measurements will provide new constraints on the gluon spin.

Acknowledgements

Thank you to Werner Vogelsang, Sassot Rodolfo and Ignacio Borsa for providing the direct photon cross section and A_{LL} calculations. Thank you to George Sterman for discussion with the principle of maximum conformality (PMC) method.

Funding information This work is supported by the Department of Energy and Research Foundation for the State University of New York.

References

[1] J. Ashman et al., *A measurement of the spin asymmetry and determination of the structure function g1 in deep inelastic muon-proton scattering*, Phys. Lett. B **206**, 364 (1988), doi:10.1016/0370-2693(88)91523-7.

[2] J. Ashman et al., *An investigation of the spin structure of the proton in deep inelastic scattering of polarised muons on polarised protons*, Nucl. Phys. B **328**, 1 (1989), doi:10.1016/0550-3213(89)90089-8.

[3] V. Yu. Alexakhin et al., *The deuteron spin-dependent structure function g1d and its first moment*, Phys. Lett. B **647**, 8 (2007), doi:10.1016/j.physletb.2006.12.076.

[4] A. Airapetian et al., *Precise determination of the spin structure function g_1 of the proton, deuteron, and neutron*, Phys. Rev. D **75**, 012007 (2007), doi:10.1103/PhysRevD.75.012007.

[5] B. Adeva et al., *Spin asymmetries for events with high p_T hadrons in DIS and an evaluation of the gluon polarization*, Phys. Rev. D **70**, 012002 (2004), doi:10.1103/PhysRevD.70.012002.

[6] HERMES Collaboration, *Leading-order determination of the gluon polarization from high-p T hadron electroproduction*, J. High Energy Phys. **08**, 130 (2010), doi:10.1007/JHEP08(2010)130.

[7] A. Zelenski et al., *Absolute polarized H-jet polarimeter development, for RHIC*, Nucl. Instr. Meth. Phys. A **536**, 248 (2005), doi:10.1016/j.nima.2004.08.080.

[8] PHENIX Collaboration, *Inclusive double-helicity asymmetries in neutral-pion and eta-meson production in $\vec{p}+\vec{p}$ collisions at $\sqrt{s}=200$ GeV*, Phys. Rev. D **90**, 012007 (2014), doi:10.1103/PhysRevD.90.012007.

[9] PHENIX Collaboration, *Gluon-spin contribution to the proton spin from the double-helicity asymmetry in inclusive π^0 production in polarized $p+p$ collisions at $\sqrt{s}=200$ GeV*, Phys. Rev. Lett. **103**, 012003 (2009), doi:10.1103/PhysRevLett.103.012003.

A. Adare et al., *Gluon-spin contribution to the proton spin from the double-helicity asymmetry in inclusive π^0 production in polarized $p+p$ collisions at $\sqrt{s}=200$ GeV*, Phys. Rev. Lett. **103**, 012003 (2009), doi:10.1103/PhysRevLett.103.012003.

[10] A. Adare et al., *Inclusive cross section and double helicity asymmetry for π^0 production in $p+p$ collisions at $\sqrt{s}=62.4$ GeV*, Phys. Rev. D **79**, 012003 (2009), doi:10.1103/PhysRevD.79.012003.

[11] L. Adamczyk et al., *Longitudinal and transverse spin asymmetries for inclusive jet production at mid-rapidity in polarized p+p collisions at* $\sqrt{s}$=200 GeV, Phys. Rev. D **86**, 032006 (2012), doi:10.1103/PhysRevD.86.032006.

[12] STAR Collaboration, *Precision measurement of the longitudinal double-spin asymmetry for inclusive jet production in polarized proton collisions at* $\sqrt{s} = 200$ GeV, Phys. Rev. Lett. **115**, 092002 (2015), doi:10.1103/PhysRevLett.115.092002.

[13] D. de Florian, R. Sassot, M. Stratmann and W. Vogelsang, *Evidence for Polarization of Gluons in the Proton*, Phys. Rev. Lett. **113**, 012001 (2014), doi:10.1103/PhysRevLett.113.012001.

[14] E. R. Nocera, R. D. Ball, S. Forte, G. Ridolfi and J. Rojo, *A first unbiased global determination of polarized PDFs and their uncertainties*, Nucl. Phys. B **887**, 276 (2014), doi:10.1016/j.nuclphysb.2014.08.008.

[15] PHENIS Collabortion, *Inclusive cross section and double-helicity asymmetry for* π^0 *production at midrapidity in* $p+p$ *collisions at* $\sqrt{s} = 510$ GeV, Phys. Rev. D **93**, 011501 (2016), doi:10.1103/PhysRevD.93.011501.

[16] STAR Collaboration, *LLongitudinal double-spin asymmetry for inclusive jet and dijet production in pp collisions at* $\sqrt{s} = 510$ GeV, Phys. Rev. D **100**, 052005 (2019), doi:10.1103/PhysRevD.100.052005.

[17] K. Adcox et al., *PHENIX detector overview*, Nucl. Instr. Meth. Phys. A **499**, 469 (2003), doi:10.1016/S0168-9002(02)01950-2.

[18] L. Aphecetche et al., *PHENIX calorimeter*, Nucl. Instr. Meth. Phys. A **499**, 521 (2003), doi:10.1016/S0168-9002(02)01954-X.

[19] K. Adcox et al., *PHENIX central arm tracking detectors*, Nucl. Instr. Meth. Phys. A **499**, 489 (2003), doi:10.1016/S0168-9002(02)01952-6.

[20] Y. Akiba et al., *Ring imaging Cherenkov detector of PHENIX experiment at RHIC*, Nucl. Instr. Meth. Phys. A **433**, 143 (1999), doi:10.1016/S0168-9002(99)00319-8.

[21] M. Allen et al., *PHENIX inner detectors*, Nucl. Instr. Meth. Phys. A **499**, 549 (2003), doi:10.1016/S0168-9002(02)01956-3.

[22] A. A. Poblaguev, A. Zelenski, G. Atoian, Y. Makdisi and J. Ritter, *Systematic error analysis in the absolute hydrogen gas jet polarimeter at RHIC*, Nucl. Instr. Meth. Phys. A **976**, 164261 (2020), doi:10.1016/j.nima.2020.164261.

[23] PHENIX Collaboration, *Measurement of neutral mesons in p+p collisions at* $\sqrt{s} = 200$ GeV *and scaling properties of hadron production*, Phys. Rev. D **83**, 052004 (2011), doi:10.1103/PhysRevD.83.052004.

[24] S. Catani, M. Fontannaz, J.-P. Guillet and E. Pilon, *Cross section of isolated prompt photons in hadron-hadron collisions*, J. High Energy Phys. **05**, 028 (2002), doi:10.1088/1126-6708/2002/05/028.

[25] S. Dulat et al., *New parton distribution functions from a global analysis of quantum chromodynamics*, Phys. Rev. D **93**, 033006 (2016), doi:10.1103/PhysRevD.93.033006.

[26] M. Klasen and F. König, *New information on photon fragmentation functions*, Eur. Phys. J. C **74**, 3009 (2014), doi:10.1140/epjc/s10052-014-3009-x.

[27] P. Nason, *A New Method for Combining NLO QCD with Shower Monte Carlo Algorithms*, J. High Energy Phys. **11**, 040 (2004), doi:10.1088/1126-6708/2004/11/040.

[28] S. Frixione, P. Nason and C. Oleari, *Matching NLO QCD computations with parton shower simulations: the POWHEG method*, J. High Energy Phys. **11**, 070 (2007), doi:10.1088/1126-6708/2007/11/070.

[29] S. Alioli, P. Nason, C. Oleari and E. Re, *A general framework for implementing NLO calculations in shower Monte Carlo programs: the POWHEG BOX*, J. High Energy Phys. **06**, 043 (2010), doi:10.1007/JHEP06(2010)043.

[30] T. Ježo, M. Klasen and F. König, *Prompt photon production and photon-hadron jet correlations with POWHEG*, J. High Energy Phys. **11**, 033 (2016), doi:10.1007/JHEP11(2016)033.

[31] M. Klasen, C. Klein-Bösing and H. Poppenborg, *Prompt photon production and photon-jet correlations at the LHC*, J. High Energy Phys. **03**, 081 (2018), doi:10.1007/JHEP03(2018)081.

[32] D. de Florian, R. Sassot, M. Stratmann and W. Vogelsang, *Global Analysis of Helicity Parton Densities and their Uncertainties*, Phys. Rev. Lett. **101**, 072001 (2008), doi:10.1103/PhysRevLett.101.072001.

[33] D. de Florian, G. Agustín Lucero, R. Sassot, M. Stratmann and W. Vogelsang, *Monte Carlo sampling variant of the DSSV14 set of helicity parton densities*, Phys. Rev. D **100**, 114027 (2019), doi:10.1103/PhysRevD.100.114027.

[34] M. Cacciari, G. P. Salam and G. Soyez, *The anti-k_t jet clustering algorithm*, J. High Energy Phys. **04**, 063 (2008), doi:10.1088/1126-6708/2008/04/063.

[35] G. D'Agostini, *Improved iterative Bayesian unfolding*, arXiv:1010.0632.

[36] CMS Collaboration, *Measurement of the inclusive jet cross section in pp collisions at $\sqrt{s} = 7$ TeV*, Phys. Rev. Lett. **107**, 132001 (2011), doi:10.1103/PhysRevLett.107.132001.

[37] PHENIX Collaboration, *Measurement of charged pion double spin asymmetries at midrapidity in longitudinally polarized $p+p$ collisions at $\sqrt{s} = 510$ GeV*, Phys. Rev. D **102**, 032001 (2020), doi:10.1103/PhysRevD.102.032001.